Caliphate Journal of Science & Technology (CaJoST)

ISSN: 2705-313X (PRINT); 2705-3121 (ONLINE) Research Article

Open Access Journal available at: https://cajost.com.ng/index.php/files and https://www.ajol.info/index.php/cajost/index

DOI: https://dx.doi.org/10.4314/cajost.v6i2.4

Article Info

Received:19th February 2024

Revised: 24th March 2024

Accepted: 3rd April 2024

[1]Department of Chemistry, Sokoto State University, Sokoto, Nigeria.
[2]Department of Pure and Environmental Chemistry, Usmanu Danfodiyo University, Sokoto, Nigeria.
[3]Department of Energy and Applied Chemistry, Usmanu Danfodiyo University, Sokoto, Nigeria.
[4]School of Chemical Engineering, Universiti Sains Malaysia, Penang, Malaysia.
[5]Central Advanced Science Research and Analytical Services, Usmanu Danfodiyo University, Sokoto, Nigeria.

***Corresponding author's email:**
yakubu.muhammadsahabi@ssu.edu.ng

Cite this: *CaJoST*, 2024, 2, 159-169

Cracking of Used Engine Oil to Gasoline-Like Fuel Using Iron Oxide Nanoparticles Supported on HZSM-5

Yaquba M. Sahabi [*1,3], Abdullahi M. Sokoto[2], Misbahu L. Mohammed[3], Abdul Rahman Mohammed[4], Mudassir Abubakar[1], Fatima M. Sahabi[1], Yahaya Nasiru[1], Kasimu Abubakar[1], and Samira S. Adamu[5]

Every day, large amount of used engine oil (UEO) is produced, which has major environmental issues due to its hazardous contaminants. UEO contains high percentage of higher molecular weight hydrocarbons that can be turned into valuable fuel products. Catalytic cracking of UEO oil into gasoline-like fuel using iron oxide nanoparticles over HZSM-5 support was investigated. The Fe_3O_4 nanoparticles was synthesised via the one-spot method using iron (III) chloride hexahydrate ($FeCl_3.6H_2O$) and iron (II) chloride tetrahydrate ($FeCl_2.4H_2O$) as precursors, while the HZSM-5 was synthesized using $Al_2(SO_4)_3.18H_2O$ and Na_2SiO_3 as sources of alumina and silica, respectively. The catalysts properties were investigated by XRD, FTIR, EDXRF, and TGA methods. The UEO was cracked in a fixed stainless-steel batch reactor at 400 °C for 1h with and without the catalyst. ASTM standard procedures, gas chromatography coupled with mass spectrometry (GC-MS), and Fourier transformed infrared spectroscopy (FTIR) were used to examine the fuel properties, molecular profile, and functional groups respectively, of the raw UEO and cracked liquid products. The results of GC-MS showed that the 10 wt.% Fe_3O_4/HZSM-5 catalyst is 86.04% selective towards $C_5 – C_{10}$ hydrocarbons, 63.16% selective towards olefins, and 18.42% selective towards aromatics. The high selectivity of the catalyst towards lighter hydrocarbons could be attributed to the pore size distribution of HZSM-5, which offers active sites for catalytic cracking. The fuel properties of the liquid products obtained using catalyst were found to be very similar to those of standard gasoline. Based on the results of the molecular profile and fuel properties, it was concluded that Fe_3O_4/HZSM-5 is a promising catalyst for cracking UEO, and the fuel obtained could be used directly in spark-ignition engines without any negative impact on engine performance.

Keywords: Engine oil, Nanoparticles, Iron oxide, Gasoline.

1. Introduction

The increase in energy demand, stringent emission laws, and depletion of petroleum resources have led the researchers to find alternative fuels for internal combustion engines. One of the most common petroleum products in use today is engine oil. It is used in industrial machines, automobiles, and all mechanical equipment (Makvisai, 2016). The primary functions of engine oil include lubrication of the engine's metal parts against the effects of friction (such as wear, tear, corrosion, etc.), cooling of the combustion cycles, cleaning the engine from combustion residues, and removal of worn-out heavy metals (Mishra *et al*., 2021; Sánchez-Alvarracín *et al.,* 2021). Engine oil is conventionally obtained from crude oil, and it consists of an average of about 80 – 90% base oil and about 10 – 20% chemical additives and other compounds (Boadu *et al*., 2019).

Over time, engine oil undergoes complex aging process where the base oil as well as the additives degrade, its physical and chemical properties become unsuitable for further use. The primary factors of engine oil degradation include oxidation, decomposition of both base oil and additives, and contamination (due to soot, water, ethylene glycol, and metal wear) (Mishra, 2021; Sánchez-Alvarracín, 2021). Once the used engine oil (UEO) becomes unusable, it is considered hazardous (Yu *et al.,* 2023) and thus, to improve on the mechanical performance, this degraded oil needs to be replaced by new lubricating oil (Boadu *et al*., 2019; Mishra *et al*., 2021; Sánchez-Alvarracín *et al.,* 2021). On the

other hand, UEO contains a high percentage of higher molecular weight hydrocarbons in its chemical composition such as aromatic, alkanes and alkenes (Boadu *et al.,* 2019). High volume of UEO can be turned into valuable products by refining, cracking, and other treatment processes. Therefore, how to recover high-quality hydrocarbon fuel from UEO and reduce its harm to the environment has become a research hotspot (Ramanathan and Santhoskumar, 2020). Finding an appropriate catalyst that can modify the reaction parameters of the process to lower the temperature and time of the reaction has been the focus of recent studies.

Over the years, HZSM-5 has been an efficient cracking catalyst due to its controllable acidity, large surface area, carbon deposition resistance and regular 10 membered ring pore structure (Zhang *et al.,* 2020). The medium pore HZSM-5 (SiO_2/Al_2O_3 range = 25 – 30) has been found to be highly selective toward C_5 – C_{12} hydrocarbons which corresponds to gasoline fractions. They are also known to promote cracking and deoxygenation reactions that leads to C_2 – C_4 olefin intermediates which condensate to aromatics, naphthenes and isoparaffins (Vu and Armbruster, 2019; Valle *et al.,* 2022). Iron-based nanomaterials possess interesting chemical and physical properties that are very different from the corresponding bulk phase, which enable them to serve as very effective catalytic agents for a variety of reactions. High specific surface area of the particles, efficient dispersion of the catalyst within the reaction medium and the ease of recovery through magnetic separation are some of the benefits of utilizing these materials. Iron (II, III) oxide nanoparticles (Fe_3O_4-NPs) catalyst have been reported to be highly selective towards olefins production, one of the most important constituents of gasoline (Wei *et al.,* 2017). The lower olefins generated on iron-based catalyst can diffuse to HZSM-5 acid sites and undergo acid catalyzed polymerization, isomerization, and aromatization reactions. Therefore, the combination of Fe_3O_4-NPs and HZSM-5 can shift the product distribution towards paraffins, olefins, naphthenes, aromatics and gasoline-range hydrocarbons. Therefore, the thrust of the present study is to develop an efficient catalyst with improved selectivity for the conversion of UEO to gasoline-like fuel.

2. Materials and Methods

2.1 Materials

UEO was collected at Total Automobile Lube Workshop, Western Bypass, Sokoto, Nigeria. The UEO was collected in a new and cleaned gallon directly from the car engine after the vehicle has been driven for an approximate range of 2000 km. Prior to the cracking, the UEO sample was filtered to remove carbon soot and other solid impurities such that the size of any remaining particulates was less than 50 µm. Aluminium sulphate octadecahydrate [$Al_2(SO_4)_3.18H_2O$], sodium silicate (Na_2SiO_3), Iron (III) chloride hexahydrate ($FeCl_3.6H_2O$, 31.62 g) and iron (II) chloride tetrahydrate ($FeCl_2.4H_2O$, 12.54 g), sulphuric acid (H_2SO_4), hydrochloric acid (HCl), and sodium hydroxide (NaOH) were purchased from Sigma-Aldrich.

2.2 Methods

2.2.1 Synthesis of Fe_3O_4 Nanoparticles

The Fe_3O_4 nanoparticles was prepared by a one-pot synthesis method. A mixture of iron (III) chloride hsexahydrate ($FeCl_3.6H_2O$, 31.62 g) and iron (II) chloride tetrahydrate ($FeCl_2.4H_2O$, 12.54 g) was added to a solution of hydrochloric acid (0.41 mol/dm^3, 150 cm^3) with continuous stirring until a clear solution is formed. In the solution, sodium hydroxide (1.5 mol/dm^3) was added in dropwise with constant stirring at 60 °C until an instant black precipitate is generated. The pH value of final suspension was maintained at 10. The resulting suspension was stirred for about 1h using hot plate magnetic stirrer. The product formed was separated by a magnet and then washed several times with distilled deionized water to obtain Fe_3O_4 nanoparticles. The freshly made nanoparticles was dried overnight at 60 °C (Wei *et al.,* 2017; Aragaw *et al*., 2021).

$$FeCl_2.4H_2O + 2FeCl_3.6H_2O + 8NaOH \longrightarrow Fe_3O_4 + 8NaCl + 20H_2O$$

2.2.2 Synthesis of HZSM-5

First, solution A as the source of alumina was prepared. The solution contained 26.7 g of aluminium sulphate ($Al_2(SO_4)_3.18H_2O$), 56 g of 98% sulphuric acid (H_2SO_4), and 15 cm^3 of deionized water. After that, solution B as the source of silica was prepared. The solution contained 56 g of sodium silicate (Na_2SiO_3) and 56 g of 40% (w/v) sodium hydroxide (NaOH). Solution A and Solution B were slowly mixed. The mixture was then homogenized using a magnetic stirrer at a speed of 1200 rpm for 5 minutes. The crystallization was performed in static conditions at 180 °C for 48 hours using a stainless steel teflon-lined autoclave in an air oven. The solid product was recovered by filtration, washed several times with deionized water until the pH of the decanted water was 7, and then dried overnight at 105 °C. Finally, the catalyst sample was calcined to remove the

organic template in a muffle furnace under an air flow at 530 °C for 12 hours at a heating rate of 3 °C/minute. The ZSM-5 zeolite in hydrogen form (H-ZSM-5) was obtained through ion exchange with an aqueous NH_4NO_3 solution. (Niu *et al.,* 2017).

2.2.3 Catalyst Doping

The doping of 10 wt.% Fe_3O_4 on HZSM-5 was performed by mixing a solution containing 10 g of the Fe_3O_4 nanoparticles with 90 g HZSM-5 catalyst support on a magnetic stirrer at 1000 rpm for 15 min. After doping, the catalyst sample was dried at 105 °C for 4 h and calcined at 700 °C for 4 h (Wei *et al.,* 2017).

2.2.4 Catalyst Characterization

FTIR analysis was carried out to confirm the mordenite framework inverted (MFI) structure of the synthesized HZSM-5. The contents of the 10 wt.% Fe_3O_4/HZSM-5 were analysed using the energy dispersive X-ray fluorescence technique (EDXRF). The X-ray diffraction (XRD) pattern of Fe_3O_4 nanoparticles and HZSM-5 were identified using a Bruker D8 Discover diffractometer equipped with a copper tube (l = 0.15418 nm), 40 kV voltage, 40 mA, and a VANTEC-500 2-D detector. The thermal stability of the Fe_3O_4/HZSM-5 catalyst was determined by thermogravimetric analysis (TGA) and differential thermal analysis (DTA) using a TG/DTA analyzer (PL-STA-1640).

2.2.5 Cracking of the Used Engine Oil

The cracking of the UEO was carried out in a fixed bed stainless steel reactor equipped with a pressure gauge. The composite catalyst (1 g) was placed on the catalyst bed and the UEO (100 cm^3) was poured into the reactor. The reactor was closed tightly and then mounted on a tubular-electric furnace equipped with thermo couples. The condenser inlet was then connected to the reactor outlet, and all the reaction conditions were set (temperature 400 ºC and time 1h). After the completion of the reaction, the outlet valve was gradually opened to vent out the vapour products. The product was condensed using the water condenser and was collected at the bottom of the condenser for analysis.

2.2.6 Characterization of UEO and Liquid Product

ASTM standard methods were followed to determine the fuel properties of the liquid product, while GC-MS and FTIR were used to examine the molecular profile and functional groups respectively, of the UEO and liquid products.

3. Results and Discussion

3.1 Fourier Transform Infrared of HZSM-5

FTIR offers quantitative and qualitative analysis for organic and inorganic samples. FTIR identifies chemical bonds in a molecule by producing an infrared absorption spectrum. The spectra produce a profile of the sample, a distinctive molecular fingerprint that can be used to screen and scan samples for many different components. In order to confirm the mordenite framework inverted (MFI) structure, FT-IR analysis was carried out. Figure 1 shows the FTIR spectrum of the synthesized HZSM-5.

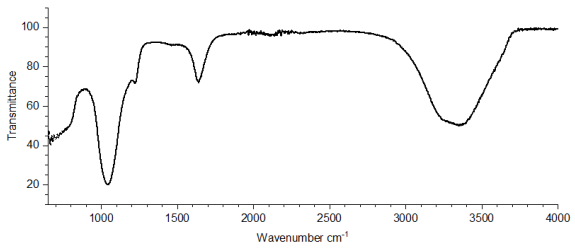

Figure 1: FTIR Spectrum of HZSM-5

The absorption bands near 794.4 and 1036.2 cm^{-1} are assigned to the internal vibrations of AlO_4 and SiO_4 tetrahedra. The absorption band near 1218.3 cm^{-1} is assigned to the asymmetric stretching of AlO_4 and SiO_4 tetrahedra in the zeolite framework. The spectrum shows bands near 794.4, 1036.2, and 1218.3 cm^{-1}, which are characteristics of the ZSM-5 framework (Jia *et al*., 2020). The broad absorption band observed around 3354.6 cm^{-1} which was assigned to the stretching vibration of the O–H bond in silanol groups (Si–O–H) but could also be due to adsorbed water molecules on the surface of silica (Smail *et al.,* 2019). The absorption band at 1634.4 cm^{-1} was attributed to the O–H bending vibration of the Si–O–H group and adsorbed water molecules (Song *et* al., 2018; Smail *et al.,* 2019). The result of FTIR agrees with those obtained by Song *et al*. (2018) and Jia *et al*. (2020) for hierarchical ZSM-5 and nano-ZSM-5, respectively.

3.2 Energy dispersive x-ray fluorescence of 10 wt.% Fe_3O_4/HZSM-5

EDXRF is designed to analyze groups of elements simultaneously. The EDXRF method was used to determine the oxide composition of all the nanoparticles, HZSM-5, and various percentages of nanoparticles on HZSM-5. The results are displayed in Figure 2.

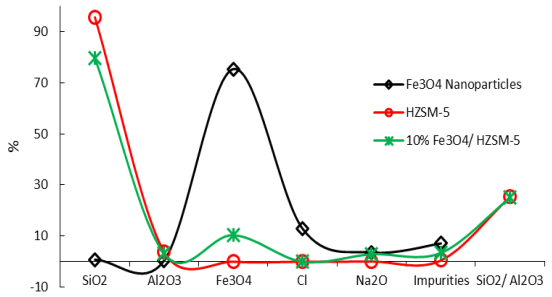

Figure 2: Composition of 10 wt.% Fe_3O_4/HZSM-5

From the EDXRF results in Figure 2, the major oxides/elements present in the synthesized catalysts are Fe_3O_4, SiO, Al_2O_3, Cl, and their respective promoter oxides. It can also be observed from the results that the HZSM-5 has a high SiO_2 content, which is a characteristic of the MFI zeolite family. The SiO_2/Al_2O_3 ratio of the HZSM-5, which is an important parameter that is used to determine the catalytic activity, was also found to be 25.32. It was also noted from the figure that, though the HZSM-5 was impregnated with the Fe_3O_4 nanoparticles, the SiO_2/Al_2O_3 ratio was maintained.

3.3 X-Ray Diffraction of HZSM-5 and Fe_3O_4 Nanoparticles

X-ray diffraction is a non-destructive analytical technique used to analyse physical properties such as phase composition, crystal structure, crystallite size, lattice strain, and orientation (Nano, 2019). The XRD analysis was performed to analyse the crystal structure of the HZSM-5 and to estimate the particle sizes of the Fe_3O_4 nanoparticles. Figures 3 and 4 showed the XRD patterns of neat HZSM-5 and Fe_3O_4, respectively.

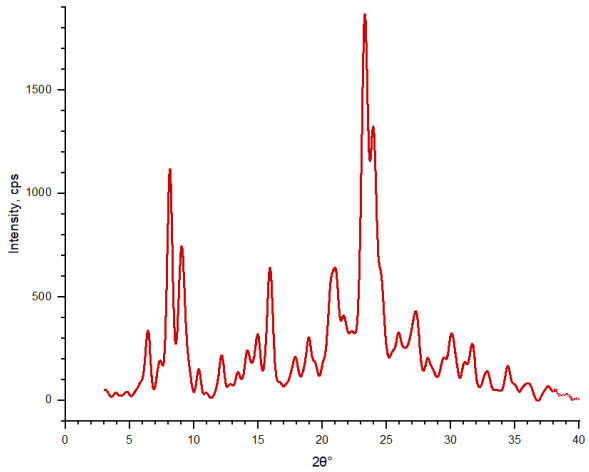

Figure 3: XRD Diffractogram of HZSM-5

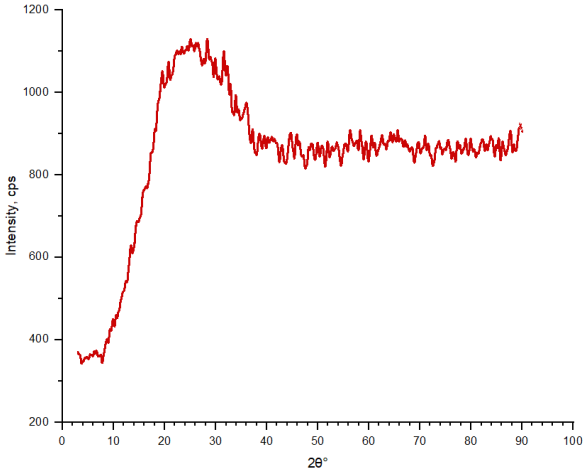

Figure 4: XRD Diffractogram of Fe_3O_4 Nanoparticles**.**

Table 1: 2θ° angles, their corresponding FWHM and size of the Fe_3O_4 nanoparticles

Angle, 2θº	FWHM°	Crystal Size (nm)
25.141560	0.1000	12.57
28.473981	0.1000	15.79
31.925417	0.1000	16.34
44.660027	0.1000	19.50

Figure 3 displayed sharp peaks at 2θ° range of 7 - 9° and 22 - 25° which are typical of the highly crystalline Mordenite Framework Inverted (MFI) structure (Huang *et al*., 2019; Bian *et al.,* 2020; Jia *et al.,* 2020). The appearance of peaks at 2θ° = 8.15, 9.09, 16.01, 23.23, 23.96 and 29.96 is attributed to the 101, 200, 301, 501, 303 and 503 crystalline nature of the HZSM-5. The figure also showed peaks that are identical to peaks of HZSM-5 that have been synthesised by Smail *et al.* 2019 and Rahmiyati, *et al*. 2019 for hierarchical ZSM-5 zeolite, uniform mesoporous ZSM-5 catalyst, and ZSM-5 catalyst, respectively. The results are also in harmony with those obtained Chen *et al*. 2021 and Sabarish and Unnikrishnan (2019) for ZSM-5 molecular sieve and hierarchical ZSM-5, respectively.

Figure 4 shows the XRD pattern of the synthesised Fe_3O_4. The Figure display intense peaks at the 2θº values of 25.14º (101), 28.47º (110), 31.93º (200) and 44.66º (211) which correspond to the pattern of highly crystalline iron oxide nanoparticles. The particle size was estimated from the full width at half maximum (FWHM) of the four strongest reflections of the peaks using the Scherrer approximation equation, which assumes the small crystalline size to be the cause of line broadening (Gobinath *et al*., 2023; Kaleem *et al.,* 2024).

$$D = \frac{K\lambda}{\beta cos\ \theta}$$

Where: K is constant = 0.9, λ = wavelength in Å, β = full-length at half maximum, θ = Bragg's differential angle.

Based on Scherrer's equation, the crystals' size was 12.57 nm, 15.79 nm, 16.34 nm and 19.50 nm. Table 1 shows the various 2θ° angles, their corresponding FWHM, and the size of the Fe_3O_4 nanoparticles. These confirm the crystalline nature of the iron oxide nanoparticles. Outcomes of this study are consistent with prior research on iron oxide nanoparticles reported by Kaleem *et al.* (2024), Ahmadi and Izanloo, (2023), and Alothman, (2024).

3.4 Thermogravimetric Analysis

TGA is a method of thermal analysis in which changes in the physical and chemical properties of materials are measured as a function of increasing temperature (with a constant heating rate) or as a function of time (with a constant temperature and/or constant mass loss) (Nasrollahzadeh *et al.,* 2019). The thermal decomposition of the synthesised catalyst was studied using the thermogravimetric method. Figure 5 displays the thermogram of the synthesised Fe_3O_4/HZSM-5 catalyst, demonstrating the weight loss of the catalyst vs. temperature.

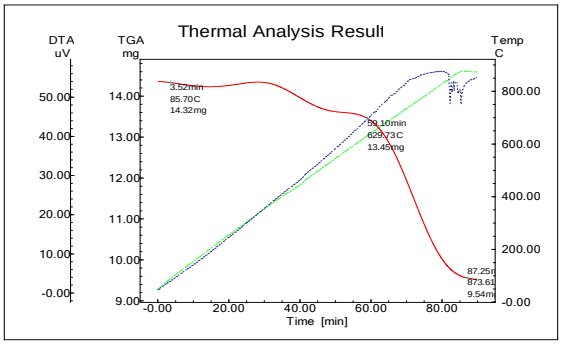

Figure 5: TGA and DTA Graph of 10 wt.% Fe_3O_4/HZSM-5 Catalyst.

The thermogram shows two distinct changes in the weight of the Fe_3O_4/HZSM-5 catalyst during the thermal analysis. At the onset of the analysis, there was a mild weight loss from 85.70 °C to 629.73 °C. The percentage weight loss recorded at this stage was 6.08%. This weight loss is associated with the dehydration and volatilization of low molecular weight organic substances. The second stage shows moderate weight loss, and it commenced from a temperature of 629.73 °C to 873.61 °C. The percentage weight loss recorded in this stage was 29.07% and this is attributed to the decomposition of Fe_3O_4 into FeO and Fe_2O_3. The severe and rapid weight loss in the second stage could also be attributed to the loss of inorganic impurities. After the second stage, the curve stabilised which indicates the end of thermal decomposition. The thermal analysis result showed that a sizable portion of the Fe_3O_4/HZSM-5 catalyst remained stable above 800 °C. This led to the conclusion that the synthesised catalyst can serve effectively as a cracking catalyst within the temperature range of 400 – 450 °C.

3.5 Molecular Composition of Raw and Cracked UEO

The percentage carbon range and PONA (paraffins, olefins, naphthenes and aromatics) composition in the liquid products obtained are shown in Figures 6 and 7, respectively.

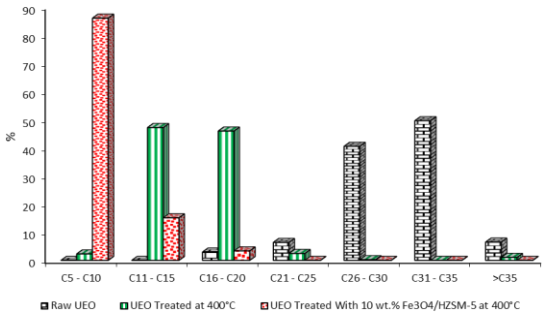

Figure 6: Percentage Carbon Range Selectivity of 10 wt.% Fe_3O_4/HZSM-5 Catalyst.

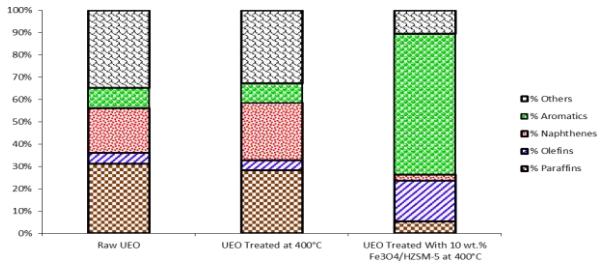

Figure 7: Percentage PONA Selectivity of 10 wt.% Fe_3O_4/HZSM-5 Catalyst.

It can be seen from Figures 6 and 7 that the raw UEO is comprised of mainly C_{26} – C_{35} organic compounds, which are dominated by paraffins and naphthenes. The results also showed that the UEO contains significant amounts of oxygenates and halides that arise from the oxidation/degradation of base oil/additives. After thermal treatment, the liquid product obtained was found to consist mainly of C_{11} – C_{20} organic compounds, with a PONA composition very identical to that of the raw UEO. However, the use of iron oxide nanoparticles over HZSM-5 for thermal treatment has significantly influenced product distribution, leading to the formation of lighter hydrocarbons with a carbon atom range of C_5 – C_{10}. The increased in lower carbon number

selectivity of the catalyst could be attributed to the pore size distribution of the HZSM-5, where larger molecules in the UEO can enter and interact with the Lewis and Bronsted acid sites in the pore, thus leading to C – C bond breakage and light components with lower carbon numbers being generated (Gong, 2022). Also, the use of catalyst has greatly shifted the PONA distribution of the UEO towards olefins and aromatics. These results indicate the conversion of larger molecules of UEO to lighter hydrocarbon components, and the subsequent formation of olefins and aromatics through cracking and aromatization occurred during the process. The production of lighter component sand subsequent elimination of impurities by Fe_3O_4/HZSM-5 represent a potentially high value fuel that is very similar to gasoline in terms of physical and chemical properties. The Lewis and Bronsted acid sites of the Fe_3O_4/HZSM-5 catalyst and the excellent pore structure stimulated catalytic activity, which selectively converted UEO into high value gasoline-like fuel with a low oxygen content through hydrogen transfer, catalytic cracking, and deoxygenation (Gong *et al.,* 2023). The Fe_3O_4/HZSM-5 catalyst has also facilitated the conversion of long-chain hydrocarbons in the UEO to much lighter and more valuable hydrocarbons.

3.6 Fourier Transform Infrared (FTIR) of Raw and Cracked UEO

Fourier transform infrared (FTIR) spectroscopy is an important analytic technique that detects various characteristic functional groups present in the produced fuel samples (Thanikachalam and Karthikeyan, 2020). Upon interaction of the infrared radiation with the fuel sample, a chemical bond can absorb the infrared radiation in a specific wavelength range, regardless of the structure of the rest of the molecules in the fuel sample (Thanikachalam and Karthikeyan, 2020). Beside functional groups from the produced fuel samples, FTIR analysis allows the detection of contaminants and impurities present (Pinheiro *et al.,* 2017). The FTIR spectra of the raw and cracked UEO are shown in Figure 8.

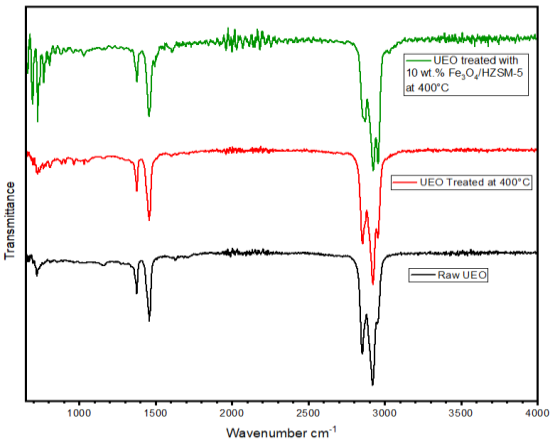

Figure 8: FT-IR Spectra

The FT-IR spectrum of raw UEO and products was recorded in the frequency range of 4000 – 650 cm^{-1}. From Figure 8, the spectra of raw UEO and products are comparably similar. The C – H stretching vibrations of alkanes (paraffins) were detected in the frequency range of 2990 – 2850 cm^{-1} in both the raw UEO and products. The presence of strong intensity peaks indicates that the paraffin content is high across all the samples. The strong peaks displayed at 2250 – 2100 cm^{-1} and 1625 – 1440 cm^{-1} frequencies represent the C=C stretching vibration in olefins and aromatics, respectively. The aromatics and olefins as constituents of the gasoline-like fuels under study were ensured by the appearance of some medium intensity peaks within the frequency range of 840 – 600 cm^{-1} due to =C-H bending (out plane) vibration. The FT-IR spectra analysis revealed all the samples exhibit a $-NO_2$ functional group at 1390 – 1300 cm^{-1}, which could be due to a nitromethane fuel additive. Thus, it may be inferred that the crude understudy contained long chain paraffins as the major components and the aromatics, olefins and oxygenate as the least concentrated components.

3.7 Fuel Properties of Raw and Cracked UEO

The properties of a fuel used for engines are important because they must be suitable for the engine to operate. In addition, these properties also serve as indicators of how the fuel will burn in the engine's combustion chamber. Therefore, these properties can be used to determine whether the fuel is suitable for use in the engine or otherwise (Suiuay *et al.,* 2023). The fuel properties of a typical gasoline fuel include octane numbers, lower heating value (LHV), viscosity, flash point, cloud point, pour point, sulphur content, and carbon residue. The fuel properties were determined in accordance with American Standard for Testing Materials (ASTM) procedures for petroleum products.

Table 2: Fuel Properties of Raw and Cracked UEO

Parameter	Raw UEO	UEO Treated at 400ºC	UEO Treated with 10 wt.% Fe_3O_4/HZSM-5 at 400ºC
Specific Gravity	0.91	0.88	0.79
Kinematic Viscosity (mm^2/Sec)	67	2.71	1.95
Lower Heating Value (KJ/kg)	79,063	47,749	42,024
Carbon Residue (wt.%)	2.76	1.15	0.35
Cloud Point (ºC)	-9	-17	-27
Flash Point (ºC)	192	13	-19
Auto ignition Temperature (ºC)	397	283	254
Octane Number	-	58	89
Sulphur Content (wt.%)	ND	ND	ND
Water Content (wt.%)	0.85	ND	ND

ND = Not Detected

Specific gravity (or relative density) is a measure of the density of an object compared to that of a reference material, and it is a dimensionless quantity. The fuel injection system of an engine operates based on the volume metering system. The higher the specific gravity of a fuel, the greater the mass of fuel injected into the engine, and hence more power and emissions. The specific gravities for the raw and treated UEO are shown in Table 2. It can be seen from the figure that the specific gravities of all the products obtained using the 10wt.% Fe_3O_4/HZSM-5 at 400 ºC catalyst is within the ASTM value of 0.75 – 0.85 for gasoline fuel. The specific gravity of the fuel products obtained is higher than 0.75 for premium motor spirit, as reported by Ivwurie et al. (2023) but lower than 0.82 for automotive gas oil, as reported by Ivwurie et al. (2023).

Viscosity is a fuel property which affects the handling, flow, pumping and burning of fuel products. It is a temperature dependent parameter and is defined as measure of fuel resistance to flow. Fuel viscosity is an important parameter to be considered when fuels are carburated or injected into combustion chamber. If viscosity is too low, the fuel will flow too easily and will not maintain a lubricating film between moving and stationary parts in the carburettor or pump. Low viscosity will also influence the fuel quality, giving it a low heating value. If viscosity is too high, it may lead to poor atomization of the fuel into small droplets to achieve good vaporization and combustion (Thahir, et al 2019). Fuels which have higher viscosity do not burn fully and coke deposits may be formed in fuel carburation or injection system, as such, viscosity of fuels must be within tolerance range. The kinematic viscosities of raw UEO and products obtained are shown in Table 2. In this study, the UEO has the highest kinematic viscosity value, which is 67 mm^2/sec, whereas the thermally treated UEO at 400 ºC with and without catalyst are 2.71 and 1.95 mm^2/sec, respectively. The kinematic viscosity of all the fuels was observed to increase with an increase in the length of the hydrocarbon range. The kinematic viscosity of the fuel products obtained using the 10wt.% Fe_3O_4/HZSM-5 catalyst at 400 ºC is within the ASTM (1.3 – 2.4 mm^2/sec) acceptable range for spark ignition engines (Thahir *et al*., 2019).

The pour point is the temperature at which fuel contains so many wax crystals that hinder its free flow. This occurs when the temperature of the fuel drops below the cloud point. Pour point is a fuel parameter that affects the flow of fuel in the pipes of the engine's fuel system. A lower value means more wax crystals will be produced, thereby hindering the ability of the fuel to flow through the engine pipe. The value of the pour point obtained for raw UEO in Table 2 is very close to -25 ºC, as reported by Muhbat et al. (2021) for waste lubricating oil. However, the result is much lower than -4 ºC for waste cooking oil, as reported by Muhbat et al. (2021).The cloud point is the temperature at which a cloud or a haze of wax crystals first starts to appear in the fuel under test conditions. The cloud point is reached when the temperature of the fuel is low enough to cause wax crystals to precipitate. The cloud point is used to measure the low temperature operability of the fuel. A clogged fuel system may be the result of these crystals accumulating in the filters. It's helpful for gauging how the fuel oil really performs in the field at low temperatures. The values of the cloud point of all the fuel products in Figure 4.17 fall within the region of extremely low temperatures. This is an indication that the fuels are suitable for low and moderate temperature climates.

Flash point and auto ignition temperature are fuel parameters that measure the flammability of a fuel. Flash point and auto ignition temperature are defined as the minimum temperature at which the vapour of a fuel begins to ignite under specified test conditions with and without an external ignition source such as a flame or spark, respectively. The measurement of the flash point and auto ignition temperature of the fuel was carried out because this parameter is essential for handling, storage, and safety purposes. A higher flash point and auto ignition temperature

indicate that a fuel is safe for handling, storage, and transportation even in mild conditions of temperature. Results shown in Table 2 revealed that the flash points of raw UEO and the product obtained by thermal treatment were 192ºC and 13ºC, respectively. These high temperatures could be attributed to heavy components and higher viscosity. As a result, more heat is needed to evaporate the combustible components. This higher value indicated that raw UEO is safer than all the fuel products obtained because the higher value shows that it is less volatile, which makes it safer for transportation, handling, and storage. While the results of fuel products obtained via the use of heat and/or catalyst showed that flame hazards related to the transportation, storage, and utilisation are much higher than normally used fuels. The values of the auto ignition temperature shown in Table 2 indicate that the fuel products obtained has less tendency to auto ignite even when in contact with a surface with a temperature of 300ºC.

UEO may contain a significant amount of water resulting from coolant leaking into the engine crankcase. As water and engine oil are immiscible, water settles at the bottom, where it can cause engine rust and engine oil pump problems. The raw UEO used in this study, as well as the fuel products obtained, were found to contain no water. Although the presence of water in the used oil has been reported in many previous literatures (Kuznetsov *et al.,* 2021), the water could vaporise as steam during the heating process in the reactor and could lead to the occurrence of the steam reforming reaction of hydrocarbons. High water content in fuels is highly undesirable because it interacts with olefinic constituents to form oxygenates. The presence of sulphur compounds in fuels has a negative impact on their quality in addition to the health damage they cause. Sulphur compounds lead to pollution of the environment due to the formation of poisonous sulphur dioxides, which are later oxidised to sulphur trioxide. Additionally, this oxide contaminates the soil with acidic substances as well as shortening the life of machines when it interacts with metal surfaces through acid rain. Sulphur compounds are undesirable in fuel as they lead to the disruption of engine exhaust and corrosion problems in fuel pumping systems (Muhbat *et al.,* 2021). Therefore, estimating the concentration of sulphur compounds in petroleum products such as gasoline and diesel is necessary because of environmental legislation developed by government organisations regulating sulphur levels in oil and its derivatives (Muhbat *et al.,* 2021). Sulphur was not detected in all the samples tested in this study. This indicates that they fall into the category of less harmful fuels.

Carbon residue content in fuel is the product of unburned hydrocarbons and ash from combustion. In general, increase in carbon residue content will affect engine quality and performance. The increase in carbon residue content will alter the viscosity, colour, and cold properties, thereby shortening the lifetime of the engine oil, which in turn may lead to engine failure (Bhangwar *et al.,* 2023). The carbon residue was expressed in terms of the percentage of carbon that is left after evaporating a known quantity of fuel under specified conditions.

The results of the carbon residue test showed that the raw UEO has the highest carbon residue content, which could be as a result of carbon deposition during fuel combustion in the engine cylinder. After the treatment process, the carbon residue concentration decreased to a bearable amount in all the fuel products.

The LHV of a fuel is a gauge of its energy content. It is a measure of the energy obtained by burning a unit mass of any fuel. It is an important property used to evaluate the quality of the fuel and to calculate technical data such as thermal efficiency in an engine. The actual heating value of a fuel is measured under laboratory conditions using a bomb calorimeter with reference to standard methods. LHV is also commonly referred to as heat of combustion or net calorific value and is directly related to the chemical composition of the fuel. LHV is a useful parameter considered in regulating the amount of fuel that needs to be injected into the engine cylinder to produce the same power output. Thus, the higher the LHV, the lower the fuel consumption and vice versa. (Sarathy *et al*., 2017; Erdogan *et al.,* 2021). LHV is measured by ASTM D240, using a bomb calorimeter, and is typically reported on a mass basis, according to SI units (KJ/kg or MJ/kg) (Sarathy *et al.,* 2017). On a mass basis, the LHV is similar for fuels with similar molecular structures. For example, all paraffinic hydrocarbons from C_5 to C_{16} have LHV in the range of approximately 44,000 – 46,000 KJ/kg, while aromatics have LHV near 40,000 – 41,000 KJ/kg (Sarathy *et al.,* 2017). The LHVs tested for produced fuels are shown in Table 2. The values obtained for all the two products are similar to the heating values of conventional petroleum gasoline and gasoline-like fuel from the pyrolysis of plastic oil reported by Jahirul et al. (2022), which are within the range of 44,000 – 47,000 KJ/kg. The lower heating value obtained for raw UEO is much higher than the 49,530 KJ/kg for waste lubricating oil reported by El-Mekkawi et al. (2020). However, the LHV of the products obtained using the 10wt.% Fe_3O_4/HZSM-5 catalyst at 400ºC is similar to the

heating value (42,400 KJ/kg) for fuel products obtained from the pyrolysis of waste plastic bags reported by Pannucharoenwong *et al.* (2023). The results obtained suggest that the fuel products could be used as fuel and burned directly in gasoline engines.

Gasoline fuel quality is measured by its octane number. The property allows gasoline to resist engine knock in an engine cylinder during combustion. The term knock refers to the spontaneous and uncontrolled auto-ignition of the air-fuel mixture in spark ignition engines (Sakai and Rothamer, 2023). Knock is one of the primary barriers to increasing engine efficiency because it limits increases in compression ratio and limits operation at optimal combustion phasing at higher engine loads (Sakai and Rothamer, 2023). Higher octane numbers indicate better resistance to detonation, which encourages smooth engine operation. Octane number is an important variable in the design of the compression ratio for an internal combustion engine (Suiuay *et al.,* 2023). Many previous studies have shown that gasoline with a high-octane number makes the engine operate with less energy, exergetic efficiency, and decreased CO and NOx emissions (Khoa *et al.,* 2022). On the other hand, the use of low-octane fuel can be problematic because engines nowadays are constructed with high compression ratios, wherein high-octane gasoline fuel is required to avoid knocking. Table 2 presents the octane numbers of the liquid fuel products obtained. It was observed that products obtained using Fe_3O_4/HZSM-5 catalyst at 400ºC have the highest-octane number.

4. Conclusion

UEO possesses a huge energy value that can be recovered if treated properly. This research, therefore carried out an investigation on the conversion of UEO into gasoline-like fuel using Fe_3O_4 nanoparticles over HZSM-5 support in a fixed-bed stainless steel reactor. The liquid products obtained were analysed using GC-MS and FT-IR. The results obtained indicated that the conversion of the UEO to gasoline-like fuel over the catalyst was feasible at 400 ºC. The catalyst exhibited 86.04% UEO conversion to gasoline range hydrocarbon fuels with an increased selectivity towards olefins and aromatics. The catalysts exhibited a higher catalytic performance due to its high surface area, pore size and volume, strong acidity, good dispersion in the reaction medium, and metal-support interaction. The overall study suggests that the iron oxide nanoparticles with HZSM-5 support could be a suitable catalyst for the enhanced and cost effective synthesis of highly sustainable gasoline fuel from UEO.

Conflict of interest

The authors declare no conflict of interest.

Acknowledgements

The authors acknowledge the support of Sokoto State University, Usmanu Danfodiyo University Sokoto, and Universiti Sains Malaysia by providing funds, research facilities and internet services.

References

Ahmadi, S. and Izanloo, C. (2023). Biosynthesis of iron oxide nanoparticles at different temperatures and its application for the removal of Zinc by plant mediated nanoparticle, as an eco-friendly nanoadsorbent. *Results in Chemistry*. 6(2023) 101192. https://doi.org/10.1016/j.rechem.2023.101192

Alothman, A. A. (2024). Kinetic formation of iron oxide nanoparticles using un- and γ-irradiated singular molecular precursor of Tris(pentanedionato)iron(III) complex. *Arabian Journal of Chemistry*. 17 (2024) 105531.https://doi.org/10.1016/j.arabjc.2023.105531

Aragaw, T. A., Bogale, F. M. and Aragaw, B. A. (2021)., Iron-based nanoparticles in wastewater treatment: A review on synthesis methods, applications, and removal mechanisms. *Journal of Saudi Chemical Society*. (2021) 25. 101280. https://doi.org/10.1016/j.jscs.2021.101280

Bhangwar, S., Memon, L. A., Luhur, M. R., khan, M. A., Rind, A. A. and khan, Z. (2023). Experimental Investigation of Effects of Tertiary Fuel on Carbon Deposition and Emissions Level of Compression Ignition Engine. *South African Journal of Chemical Engineering*. 47 (2024) 291–299. https://doi.org/10.1016/j.sajce.2023.11.012

Bian, K., Zhang, A., Yang, H., Fan, B., Xu, S., Guo, X., and Song, C. (2020). Synthesis and Characterization of Fe-Substituted ZSM - 5 Zeolite and Its Catalytic Performance for Alkylation of Benzene with Dilute Ethylene. *Ind. Eng. Chem. Res.* 2020, 59, 22413−22421. https://doi.org/10.1021/acs.iecr.0c01909.

Boadu, K. O., Joel, O. F., Essumang, D. K. and Evbuomwan, B. O. (2019). A Review of Methods for Removal of Contaminants in Used Lubricating Oil. *Chemical Science International Journal*, *26*(4), 1–11. https://doi.org/10.9734/csji/2019/v26i430101

Chen, O., Liu, S., Zhang, P. and Zheng, S. (2021). Green Synthesis and Application of ZSM-5 Zeolite. *Kem. Ind*. *70*, 121–127. DOI:10.15255/KUI.2020.041

El-Mekkawi, S. A., El-Ibiari, N. N., Attia, N. K., El-Diwani, G. I., El-Ardy, O. A. and Morsi, A. K. E. (2020). Reducing the Environmental Impact of Used Lubricating Oil Through the Production of Fuels by Pyrolysis. *Environmental Nanotechnology, Monitoring and Management*, *14*, 100308. https://doi.org/10.1016/j.enmm.2020.100308

Erdoğan, S. (2021). LHV and HHV prediction model using regression analysis with the help of bond energies for biodiesel. *Fuel*, *301(2021) 121065*. https://doi.org/10.1016/j.fuel.2021.121065

Gobinath, E., Dhatchinamoorthy, M., Saran, P., Vishnu, D., Indumathy, R. and Kalaiarasi, G. (2023). Synthesis and Characterization of NiO Nanoparticles using Sesbania Grandiflora Flower to Evaluate Cytotoxicity. Results in Chemistry. 6 (2023) 101043. https://doi.org/10.1016/j.rechem.2023.101043

Gong, G., Luo, J., Sun, S., Lin J., Ma, R. and Sun, J. (2023). Dual function intensified cracking of waste engine oil to produce alkane-rich oil: Study on the synergistic effect of Fe-Co/MCM41 catalyst and microwave. *Fuel.* 332(2). https://doi.org/10.1016/j.fuel.2022.126245

Huang, H., Zhu, H., Zhang, Q. and Li, C. (2019). Effect of Acidic Properties of Hierarchical HZSM-5 on the Product Distribution in Methanol Conversion to Gasoline. *Korean Journal of Chemical Engineering.* 36(2). 210 – 216. https://DOI:10.1007/s11814-018-0209-3

Ivwurie, w., Okorodudu, E. O. and Ahworegba, V. O. (2023). Analysis of the Quality of Petroleum Products from different Retail Outlets in Ughelli North, Delta State, Nigeria. FUPRE Journal of Scientific and Industrial Research. Available online at http://fupre.edu.ng/journal. 7(2). 01-07

Jahirul, M. I., Faisal, F., Rasul, M. G., Schaller, D., Khan, M. M. K. and Dexter, R. B. (2022). ScienceDirect Automobile fuels (diesel and petrol) from plastic pyrolysis oil — Production and characterisation. *Energy Reports*, *8*, 730–735. https://doi.org/10.1016/j.egyr.2022.10.218

Jia, Y., Shi, O., Ding, C. and Zhang, K. (2020). Synthesis, Characterization, and Catalytic Application of Hierarchical Nano-ZSM-5 Zeolite. *RSC Advances.* 10. 29618 – 29626. https://doi.org/10.1039/D0RA06040B

Kaleem, M., Minhas, L. A., Hashmi, M. Z., Farooqi, H. M. U., Waqar, R., Kamal, K., Aljaluod, R. S., Alarjani, K. M. and Mumtaz, A. S. (2024). Biogenic synthesis of iron oxide nanoparticles and experimental modeling studies on the removal of heavy metals from wastewater. *Journal of Saudi Chemical Society*. 28 (2024) 101777. https://doi.org/10.1016/j.jscs.2023.101777

Khoa, N. X. and Lim, O. (2022). *In fluence of Combustion Duration on the Performance and Emission Characteristics of a Spark-Ignition Engine Fueled with Pure Methanol and Ethanol*. https://doi.org/10.1021/acsomega.1c05759

Kuznetsov, G. V., Volkov, R. S. and Strizhak, P. A. (2021). Determining water content in a liquid fuel by the luminosity of its droplet. *Chemical Engineering Science*. 233 (2021) 116415. https://doi.org/10.1016/j.ces.2020.116415

Makvisai, W., Promdee, K., Tanatavikorn, H. and Vitidsant, T. (2016). Catalytic Cracking of Used Lubricating Oil Over Fe/Al_2O_3 and Fe/SiO_2-Al_2O_3. *Petroleum and Coal.* 58(1). 83 – 94. ISSN 1337 – 7027

Mishra, A., Siddiqi, H., Kumari, U., Behera, I. D., Mukherjee, S., and Meikap, B. C. (2021). Pyrolysis of Waste Lubricating Oil/Waste Motor Oil to Generate High-Grade Fuel Oil: A comprehensive review. *Renewable and Sustainable Energy Reviews*, *150*(January), 111446. https://doi.org/10.1016/j.rser.2021.111446

Muhbat, S., Tufail, M. and Hashmi, S. (2021). Production of Diesel-Like Fuel by Co-Pyrolysis of Waste Lubricating Oil and Waste Cooking Oil. *Biomass Conversion and Biorefinery*. https://doi.org/10.1007/s13399-021-01569-9

Nasrollahzadeh M., Atarod M. and Sajadi SM. (2019). Green synthesis of the Cu/Fe_3O_4 nanoparticles using *Morinda morindoides* leaf aqueous extract: a highly efficient magnetically separable catalyst for the reduction of organic dyes in aqueous medium at room temperature. *Appl Surf Sci 2016*; 364:636–44. https://ui.adsabs.harvard.edu/link_gateway/2016ApSS..364..636N/doi:10.1016/j.apsusc.2015.12.209

Niu, X., Gao, J., Wang, K., Miao, Q., Dong, M., Wang, G., Fan, W., Qin, Z. and Wang, J. (2017)., Influence of crystal size on the catalytic performance of H-ZSM-5 and Zn/H-ZSM-5 in the conversion of methanol to aromatics. *Fuel Processing Technology.* 157. 99 – 107. DOI: 10.1016/j.fuproc.2016.12.006

Pannucharoenwong, N., Duanguppama, K. and Echaroj, S. (2023). ScienceDirect Improving fuel quality from plastic bag waste pyrolysis by controlling condensation temperature.

Energy Reports, *9*(February), 125–138. https://doi.org/10.1016/j.egyr.2023.05.231

Pinheiro, C. T., Ascensão, V. R., Cardoso, C. M., Quina, M. J. and Gando-Ferreira, L. M. (2017). An Overview of Waste Lubricant Oil Management System: Physicochemical Characterization Contribution for its Improvement. *Journal of Cleaner Production*, *150*, 301–308. https://doi.org/10.1016/j.jclepro.2017.03.024

Rahmiyati, L., Arita, S., Komariah, L. N., Nazarudin, N. and Alfernando, O. (2019). Synthesis, Characterization of ZSM-5 Catalyst for Catalytic Pyrolysis of Empty Fruit Bunches. *Indonesian Journal of Fundamental and Applied Chemistry*. 72 – 76. https://DOI:10.24845/ijfac.v4.12.72

Sabarish, R. and Unnikrishnan, G. (2019). Synthesis, Characterization and Evaluation of Micro/Mesoporous ZSM-5 Using Starch as Bio Template. *SN Applied Sciences.* 2019(1). 989. https://doi.org/10.1007/s42452-1036-9

Sakai, S. and Rothamer, D. (2023). 2-methyl-3-buten-2-ol-gasoline blends under premixed prevaporized conditions in a spark-ignition engine. *Combustion and Flame*, *251*, 112685. https://doi.org/10.1016/j.combustflame.2023.112685

Santhoshkumar, A. and Ramanathan, A. (2020). Recycling of waste engine oil through pyrolysis process for the production of diesel like fuel and its uses in diesel engine. *Energy*. 197 (2020) 117240. https://doi.org/10.1016/j.energy.2020.117240

Sánchez-Alvarracín, C., Criollo-Bravo, J., Albuja-Arias, D., García-Ávila, F. and Raúl Pelaez-Samaniego, M. (2021). Characterization of Used Lubricant Oil in a Latin-American Medium-Size City and Analysis of Options for its Regeneration. *Recycling*, *6*(1), 1–22. https://doi.org/10.3390/recycling6010010

Sarathy, S. M., Farooq, A. and Kalghatgi, G. T. (2017). Recent progress in gasoline surrogate fuels. *Progress in Energy and Combustion Science*, *000*, 1–42. https://doi.org/10.1016/j.pecs.2017.09.004

Smail, H. A., Rehan, M., Shareef, K. M., Ramli, Z., Nizami, A. and Gardy, J. (2019). Synthesis of Uniform Mesoporous Zeolite ZSM-5 Catalyst for Friedel-Crafts Acylation. *Chemengineering* 1–11. https://doi.org/10.3390/chemengineering3020035

Song, G., Chen, W., Dang, P., Yang, S., Zhang, Y., Wang, Y., Xiao, R., Ma, R. and Li, F. (2018). Synthesis and Characterization of Hierarchical ZSM-5 Zeolites With Outstanding Mesoporosity and Excellent Catalytic Properties. *Nanoscale Research Letter.* (2018) 13:364. Https://doi.org/10.1186/s11671-018-2779-8

Suiuay, C., Katekaew, S., Senawong, K., Junsiri, C., Srichat, A. and Laloon, K. (2023). Production of gasoline and diesel-like fuel from natural rubber scrap: Upgrading of the liquid fuel properties and performance in a spark ignition engine. *Energy*, *283*. https://doi.org/10.1016/j.energy.2023.128583

Thahir, R., Altway, A. and Juliastuti, S. R. (2019). Production of liquid fuel from plastic waste using integrated pyrolysis method with refinery distillation bubble cap plate column. *Energy Reports*, *5*, 70–77. https://doi.org/10.1016/j.egyr.2018.11.004

Thanikachalam, J. and Karthikeyan, S. (2020). Study on extraction of pollutant free flammable fuel from contaminated automobile waste lube oil. *Journal of Achievements in Materials and Manufacturing Engineering*, *100*(2), 78–84. https://doi.org/10.5604/01.3001.0014.3348

Valle, B., Palos, R., Bilbao, J. and Gayubo, A. G. (2022). Role of zeolite properties in bio-oil deoxygenation and hydrocarbons production by catalytic cracking. Fuel Processing Technology. 227(2022). 107130. https://doi.org/10.1016/j.fuproc.2021.107130

Vu, H. X. and Armbruster, U. (2019). Designing Hierarchical ZSM-5 Materials for Improved Production of LPG Olefins in the Catalytic Cracking of Triglycerides. *Advances in Materials Science and Engineering*. Volume 2019, Article ID 3198421, 7 pages https://doi.org/10.1155/2019/3198421

Wei, J., Ge1, Q., Yao, R., Wen, Z., Fang, C., Guo, L., Xu, H. and Sun, J. (2017). Directly Converting CO_2 into a Gasoline Fuel. *Nature Communications.* 8:15174. DOI: 10.1038/ncomms15174. www.nature.com/naturecommunications.

Yu, B., Peng, Y., Gong H. and Liu, Y. (2023). Evaluation of the techno-economic and environmental performance of all-component recycling process for waste lubricating oil. Separation and Purification Technology. 312(1). https://doi.org/10.1016/j.seppur.2023.123402

Zhang, R., Zhong, P., Arandiyan, H., Guan, Y., Liu, J., Wang, N., Jiao, Y. and Fan, X. (2020). Using ultrasound to improve the sequential post-synthesis modification method for making mesoporous Y zeolites. *Front. Chem. Sci. Eng.* 2020, 14(2): 275–287. https://doi.org/10.1007/s11705-019-1905-1

